Gliders on Aperiodic Monotilings: Cellular Automata on the Hat and Spectre

James Edmond
London, United Kingdom
james@offlattice.org

The hat and spectre monotiles, discovered in 2023, tile the plane only aperiodically. Cellular automata are studied here on patches generated by finite-state transducers, so that every experiment regenerates deterministically from a small record. Within edge-adjacency semi-totalistic rules, exhaustive and evolutionary searches find only mortal travelers: gliders are absent. Guided by a reproduction of the known Penrose-tiling glider, the rule space is extended to vertex neighborhoods and to priority-table rules whose non-quiescent states are visible to neighbors. Evolutionary search then discovers gliders on both monotilings; tracked by a sliding window that regenerates the patch along the flight, they travel one million rings at constant speed and heading. All headings are quantized, to millidegrees, onto a six-spoke compass — the fast axes of the tiling's graph metric. An ablation shows both rule-space extensions are individually necessary. All results replay exactly in an accompanying interactive essay.

Keywords: cellular automata; gliders; aperiodic tilings; hat tiling; spectre tiling; Penrose tilings; evolutionary search

1. Introduction

An aperiodic monotile is a single shape whose copies tile the plane, but never periodically. Whether such a shape exists—the *einstein* problem—remained open for over half a century, until 2023: the *hat*, a 13-sided polykite, tiles the plane only aperiodically [1], and the *spectre*, found weeks later, does so without reflected copies [2]. The two tilings have been studied intensively as geometry; here they are substrates for dynamics.

This paper asks whether the monotilings support *gliders*: bounded patterns that travel indefinitely. In Conway's Game of Life [3] the glider is the elementary carrier of information, and everything Life is famous for—guns, logic gates, universal construction [4]—rests on it. On a periodic lattice, gliders are cheap in a precise sense: translation symmetry guarantees that a pattern that works once works forever, because after one period it faces an identical neighborhood. An aperiodic tiling revokes exactly this guarantee — not because local environments are

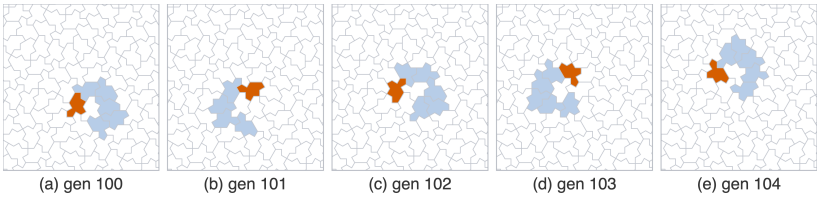

Figure 1. Five consecutive generations of a glider on the spectre tiling. Gray outlines show a patch of the spectre tiling — a tiling with no translational period; colored tiles are the non-quiescent cells of a four-state cellular automaton—one *head* cell in state 1 (vermilion) and a wake of state-3 *wing* cells (pale blue); state 2, which this rule never enters, is green where later automata use it. State colors darken toward state 1, so the ordering survives grayscale reproduction. The panels are consecutive generations (100–104 of the committed record), so each transition can be checked by hand against the rule table; the object, one of a pair launched by a two-cell seed, holds a fixed heading and advances one ring of the tiling every two generations, its handful of cells re-formed at every step on tiles it has never visited. The rule and seed are given in Section 6; the record replays live in the companion essay.

unrepeatable (every finite patch of an aperiodic tiling recurs infinitely often), but because no translation maps the tiling to itself: recurrence comes with no schedule, and surviving one environment implies nothing about the next. A moving pattern cannot translate; it must be re-formed, step by step, along a sequence of local environments that never becomes periodic. Figure 1 shows an object that does so.

The question has a history on the Penrose tilings [5]. Owens and Stepney studied Game of Life rules on the kite-and-dart and rhomb tilings and mapped their still lifes and oscillators [6]; no mobile pattern was found. The first glider on any aperiodic tiling was exhibited in 2012 [7]: a four-state automaton on the generalized Moore neighborhood whose two-cell seed travels the rhomb tiling indefinitely, overturning a conjecture—backed by a modest cash prize—that no such object could exist [8]. Its immortality is geometric. The rhomb tiling carries *de Bruijn ribbons* [9], straight bands of rhombi crossed edge to parallel edge, and the glider rides them; because rhombi are parallelograms, progress along a ribbon is monotone and the path can never close. By a different route, Bailey and Lindsey constructed automata on multigrid-derived Penrose tilings that are isomorphic to Life itself, importing its glider wholesale rather than finding one native to the tiling [10]. On the hat tiling itself, rules have been explored interactively since the year of its discovery in Trevorrow's *HatLife* [11], including a hand-designed rule whose *worms* travel across its patch; we learned of that work only after the first version of this paper was posted, and a note at the end

of Section 7 sets it beside the results below. The monotilings have no analogue of the rhomb tiling's straight rails. Goucher's mechanism therefore does not transfer, and the question becomes: can directed transport exist without rails?

Our answer is yes, and the paper is organized around how such a claim can be tested. Every experiment is a compact record— tiling family, root address, radius, neighborhood, rule, and seed— from which patch and run regenerate deterministically via the substitution-transducer machinery of Tatham [12]; classification is exact, with periods detected as exact recurrences of the full patch state. Searches are evolutionary, and their fitness functions carry structural controls that were each installed after a search exploited the objective's previous form (Section 3). Above all, the pipeline was validated before any monotiling claim was trusted: pointed at the Penrose rhomb tiling, where ground truth exists, it must and does reproduce the published glider—a reproduction that also surfaced a misprint in the published transition table—and, unaided, rediscovers gliders there at a measurable search cost (Section 4). The same compiled engine that ran every search runs in the browser: a companion interactive essay replays each committed record live, so the evidence for every figure in this paper can be watched, not merely cited (Section 8).

The contributions are as follows.

1. Machinery for cellular automata on the hat and spectre tilings in which every run is an exactly replayable record and every patch is regenerated from its address rather than shipped as geometry.

2. A scoped negative result: under edge adjacency and Generations-style rules (dying states invisible to neighbors), the monotilings support only mortal travelers—exhaustively so for two states, and a conclusion that survives a thirteenfold increase in search budget.

3. A reproduction of the published Penrose glider with a corrected transition table (the misprint is confirmed against the paper's prose, the reference implementation, and reproduction), together with blind rediscovery of gliders on that tiling, including one twice the published speed.

4. Gliders on both the hat and the spectre: population-bounded travelers flown one million rings at constant speed and heading in a sliding window, igniting from 71–89% of arbitrary two-tile seeds, with a first interaction repertoire (annihilation, nondestructive deflection, and one observed lane capture).

5. A compass law, measured exact: every mobile object travels on a fan of directions quantized to 60° (36° on Penrose P3) with one fitted offset per substrate; on the monotilings all six spokes carry measured lanes, and the fan directions are the cusp axes of the tiling's graph metric—the Penrose rails emerge as a special case.

6. An ablation showing the two rule-space extensions (the vertex neighborhood, and neighbor-visible states with conjunctive conditions) are each individually necessary, and a transferable anti-gaming methodology in which every parasite bred by a fitness function became a structural control.

Section 2 describes the substrate and engine; Section 3 the rule families, the search, and the verification standard; Section 4 the Penrose validation. Section 5 presents the monotiling results: the gliders and their verification, the compass law, interactions, ignition genericity, and the ablation. Section 6 is an atlas of the individual objects — for each, the complete rule, seed, portraits, and measured invariants, everything needed to recreate and recognize it. Section 7 discusses mechanism and prospects, and Section 8 records the reproducibility artifacts.

2. Substrate and Engine

2.1 Patches as graphs

A cellular automaton on a tiling takes the tiles themselves as cells. Following the combinatorial approach of Tatham [12], a *patch* is identified by a triple (tiling family, root tile address, radius): starting from a canonical address for the root tile, a breadth-first walk over the family's neighbor transducer enumerates every tile within the given graph distance, producing an adjacency graph in compressed sparse row form together with per-cell metadata (tile class, chirality, address, and graph distance from the root). The class records the tile's role in the substitution hierarchy — which slot of which first-level supertile it occupies, counting the transducer's context variants of the supertiles as distinct [12] — and takes one of finitely many values: 17 on the hat tiling, 10 on the spectre. The dynamics never see coordinates. Polygon geometry is computed separately, by exact arithmetic in a cyclotomic ring, and is used only for rendering and for the vertex adjacency defined below; because each tile is placed once via its breadth-first tree edge, every non-tree graph edge independently checks that two placements derived along different paths still abut, validating the transducer against the geometry.

Patch generation is deterministic: the same triple always yields the same graph, with the same cell numbering, and the cells of a radius-r patch form an index-for-index prefix of the cells of any larger patch on the same root. Every experiment in this paper is therefore stored as a small *record*—family, root, radius, neighborhood, rule, and initial cell states—from which the run regenerates exactly, in the search code and in the browser alike.

One pitfall is recorded here because correctness depends on it: an eventually periodic address whose repeating cycle touches its supertiles' boundary describes a *cone* rather than the plane, and the transducer silently glues the seam, corrupting adjacency near the seed. Root addresses are therefore chosen with *eventually interior* cycles, and patch generation flags any seam-crossing cell; every run in this paper has an empty flag set.

2.2 Two neighborhoods

Two adjacency relations generalize naturally from grid automata to polygonal tilings: tiles sharing an edge (the generalized von Neumann neighborhood [13] — four neighbors on the square grid) and tiles sharing at least one boundary vertex (the Moore neighborhood [14], as generalized by Owens and Stepney [6] — eight on the square grid, the neighborhood of Life). Edge adjacency is what the neighbor transducer provides natively. Vertex adjacency is computed at patch-generation time by collecting each tile's placement vertices in exact arithmetic and linking tiles that share a vertex value; equality is exact, so no tolerance parameter is involved, and the result is again a plain adjacency graph.

Neighborhood sizes are variable, which shapes the available rule families (Section 3). Under edge adjacency, interior hat-tiling cells have four to six neighbors (the reflected tiles, anti-hats, always have exactly four), spectre cells have four to seven, and Penrose rhombs and kites have exactly four. Under vertex adjacency, hat and spectre cells have six or seven neighbors, Penrose P2 cells eight to ten, and P3 cells seven to eleven.

Activity is measured in *rings*: the graph distance of a cell from the root under edge adjacency, which is also the metric of patch construction. A single vertex-adjacency step can cross more than one ring, because the tiles around a shared vertex form an edge-connected fan; the maximum ring difference across any vertex edge, the *fan margin*, is measured on each patch directly (two rings on the monotilings and P2, three on P3). Cells within the fan margin of the patch boundary have incomplete neighborhoods, and classification treats them as boundary.

2.3 Exact classification

The engine performs synchronous, double-buffered updates on the fixed graph, with a dead boundary. Runs are classified exactly. Cycle detection uses Brent's algorithm [15] over full state snapshots, so a reported period is an exact global recurrence, not a hash collision; in particular a traveling pattern cannot be misreported as periodic, because on an aperiodic substrate a mover never returns the whole patch to a previous state. A run ends in one of five outcomes: died; periodic, with exact period; reached the patch boundary; exceeded a population cap;

or still active at the horizon. Reaching the boundary both terminates faithful simulation (the infinite tiling is no longer being simulated) and serves as the explosion filter, since space-filling rules reach it in time proportional to the radius.

2.4 Flight-scale simulation: the sliding window

A monolithic patch has cost quadratic in its radius — near two million tiles at radius 768, the practical ceiling — so verification by patch growth alone cannot follow a glider far. Because a patch is only an address and a radius, the window can instead follow the object. A flight is simulated on a small window (radius 24 suffices for the gliders here); whenever the active set nears the window edge, the entire nonzero state is extracted, a fresh window is generated rooted at the leading cell's canonical address, the extracted cells are placed into it by address, and the run continues. An invariant asserted at every generation — no active cell within the fan margin plus two rings of the window edge — guarantees that every neighborhood the automaton ever reads is complete, so by induction the composite run is exactly the run on the infinite tiling. The construction is also validated directly: sliding runs reproduce monolithic runs exactly at every sampled generation.

Geometry survives the hops. Consecutive windows share thousands of tiles; matching them by address determines the rigid transform between the two window frames exactly — the rotation must lie on the tiling's finite orientation set, and this is asserted — and composing the transforms yields the object's global position and heading from launch, to floating-point precision, over arbitrarily many hops. Memory use is constant in flight distance, per-hop cost grows only logarithmically (the depth of the window's address), and every hop emits a complete record, independently replayable like any other. This is the instrument behind the million-ring measurements of Section 5; the companion essay animates the mechanism — the substrate generated just ahead of the glider as it flies.

3. Rule Families, Search, and Verification

3.1 Rule families

Variable neighborhood sizes force *semi-totalistic* rules: transitions may depend on the number of neighbors in given states, but not on their arrangement — the class the Penrose-tiling literature calls *outer totalistic* [6, 7]. Two families are used.

The first is the *Generations* family. A rule has k states: 0 is quiescent, 1 is alive, and states $2, \ldots, k-1$ are dying phases that age deterministically toward death. Only neighbors in state 1 are counted;

a dead cell becomes alive if its live-neighbor count lies in a birth set B, a live cell remains alive if its count lies in a survival set S and otherwise begins dying. For $k = 2$ this is exactly the Life-like family. Rules may additionally be *stratified* by tile class, giving each class its own (B, S) table — 17 tables on the hat, 10 on the spectre.

The second family, *priority-table rules*, removes two restrictions at once. A rule is an ordered list of rows; each row specifies an own-state (or a wildcard), a conjunction of per-state neighbor-count thresholds (for example, $n_1 \geq 1$ and $n_3 \geq 2$, where n_i counts neighbors in state i), and a next state. The first matching row fires; if none matches, the cell becomes quiescent. Two properties distinguish this family from Generations: non-quiescent states other than 1 are visible to neighbors, and conditions may require several signals jointly. The family strictly contains the Generations rules, since any exact count can be encoded by descending thresholds. Its significance for gliders is developed in Section 4.

3.2 Search

Two-state edge-adjacency rule spaces are small enough to enumerate: about 10^4 to 10^5 rules per family after excluding birth on zero neighbors, each evaluated on random soups and on small seeds and classified exactly. Roughly three quarters of the hat tiling's two-state rule space is explosive.

Larger spaces are searched by a genetic algorithm. For Generations rules the genome is one (B, S) table per tile class; for priority-table rules it is the row list itself (at most eight rows of at most two conditions), mutated by row insertion, deletion, reordering, and field edits, and recombined by one-point row splicing. Populations are initialized at random; no known rule is planted. Each genome is evaluated from a fixed bank of 13 two-cell and one-ball seeds at the patch root, neutral with respect to state roles, and scored by

$$f = \begin{cases} 0 & \text{if } P_{\max} > C, \\ d \cdot P_{\text{inner}}/P_{\max} & \text{otherwise,} \end{cases} \tag{1}$$

where d is the farthest ring reached by any state change, $P_{\max}$ is the peak population, C is a population cap, and P_{inner} is the peak population before activity first reached half the boundary distance. The ratio in equation (1) is a growth-slope probe: a bounded traveler keeps $P_{\text{inner}} \approx P_{\max}$, while a pattern that grows as it travels is discounted.

3.3 Verification, and the parasites that shaped it

A bounded pattern that reaches the boundary of one patch proves only that it traveled at least that radius. The glider criterion used

throughout is therefore *cross-radius verification*: the candidate must reach the boundary at every radius in a geometric family (48, 96, 192, 384 rings here), with flat peak population at every scale. The spacing is multiplicative because tightly spaced radii can mask slow growth.

Each term of the fitness function, and each verification control, exists because a search exploited its absence. Reward for reaching the boundary let mortal travelers pose as escapees on any patch smaller than their range (hence raw distance, and verification only across radii). The population cap alone bred ever-thinner growers that fit under it (hence the growth-slope ratio). Most strikingly, on edge-adjacency patches the table-rule search discovered *boundary sniffing*: a rule such as "any cell with $n_0 \geq 3$ becomes quiescent; otherwise state 1" ignites nothing that travels, but detects the patch boundary itself, because corner cells of a finite patch have fewer neighbors than any interior cell. The exploit scales with the patch and therefore passes cross-radius verification—the only parasite found that does. It is excluded by a *causality filter*: activity must remain inside the light cone of the seed, that is, the farthest changed ring may not exceed $d_0 + g \cdot m$, with d_0 the seed's extent, g the elapsed generations, and m the fan margin. Boundary sniffing is structurally impossible under vertex adjacency, where the minimum degree exceeds the threshold range, and none of the gliders reported below relies on it; the general lesson, that every objective breeds its parasite and every parasite must become a structural control, is one of the paper's methodological conclusions.

4. Validation on Penrose Tilings

Before trusting any search on substrates where we had no ground truth, the pipeline was pointed at the one aperiodic tiling with a peer-reviewed glider. Gliders on Penrose tilings were conjectured impossible by Trevorrow [8] and found by Goucher [7]: a four-state outer-totalistic automaton on the generalized Moore neighborhood whose head-and-tail seed travels along the de Bruijn ribbons of the P3 rhomb tiling—straight bands of rhombs crossed edge to parallel edge, whose parallelogram geometry forbids the path from ever closing. The validation had two levels: can the machinery *recognize* the known glider, and can the search *rediscover* gliders unaided at feasible cost?

4.1 Detection, and an erratum

Encoded exactly as printed, the published transition table cannot glide: no row of the table causes a change to state 1, so a head can never be reborn, and the seed dies within four generations in every orientation. Yet the paper's own prose describes exactly that event — "a new head is reborn ahead of the original one" — and only the second row can

Current state	Neighbor condition	Next state
0	$n_1 \geq 1$ and $n_2 \geq 1$	3
0	$n_1 \geq 1$ and $n_3 \geq 2$	1
1	$n_3 \geq 1$	2
1	always	1
2	always	3
any	otherwise	0

Table 1. The corrected Penrose glider automaton of [7] (states: 0 ground, 1 head, 2 tail, 3 wing; first matching row fires). The published table misprints the second row's next state as 3, under which state 1 is unreachable and the automaton supports no glider; the value 1 is confirmed by the paper's prose, by the reference implementation [16], and by reproduction.

implement it, since its conditions (a ground cell beside the head and at least two of its wings) single out the cell just ahead of the glider. Its next state must therefore be 1, not the printed 3; the reference implementation distributed with the simulator *Ready* [16] uses 1. Table 1 shows the corrected automaton; with it, the glider reproduces immediately.

With the corrected rule, a head-and-tail pair seeded across any shared edge of any tile class launches a glider (40 of 40 seedings tested), which crosses patches of radius 24 to 120 at a constant two generations per ring with peak population ten, flat at every radius. On the P2 kite-and-dart tiling the same rule instead produces *loopers*, closed orbits whose exact periods—20, 40, and, on larger patches, 200—match the published values; 40 and 200 open the published decagonal sequence $40, 200, 1240, \ldots$, whose successive periods obey $P_{n+2} = 5P_{n+1} + 6P_n$. Exactness here is meaningful: periods come from Brent recurrence of the full patch state, not from local pattern matching.

4.2 Rediscovery, and a calibration

The second level asks whether the unmodified search finds gliders where gliders exist. At modest budget (population 96, 300 generations) it does not: blind runs plateau on mortal travelers and oscillators at a quarter of the attainable fitness. Seeding one run with the known glider confirmed that the objective ranks a true glider strictly above everything the blind searches had found; the optimizer, not the fitness landscape, was the limit. At a sevenfold larger budget (population 256, 800 generations, about 1.15×10^5 genome evaluations), blind search crossed the needle: four of six independent runs produced cross-radius-verified gliders.

None of them is Goucher's. One is a *phoenix* glider whose rule gives states 1 and 2 no survival rows at all—every live cell dies each generation and the pattern is reborn ahead of itself—and which travels at one

Current state	Neighbor condition	Next state
3	$n_2 \geq 1$	1
0	$n_2 \geq 3$	0
0	$n_3 \geq 1$ and $n_2 \geq 1$	3
0	$n_3 \geq 1$ and $n_2 \geq 1$	3
0	$n_3 \geq 2$ and $n_3 \geq 2$	1
0	$n_3 \geq 2$ and $n_3 \geq 2$	2
0	$n_3 \geq 1$ and $n_0 \geq 3$	2
0	$n_3 \geq 1$ and $n_0 \geq 3$	2
any	otherwise	0

Table 2. The phoenix glider's automaton (first matching row fires; the final row is the default; grayed rows are inert in the sense of Section 6). Seed: state 2 on the root thick rhomb, state 3 on a thin neighbor. States 1 and 2 have no survival rows — every live cell dies each generation and the anatomy is reborn ahead of itself, one ring per generation. Row two, dead-to-dead, is nonetheless essential: it suppresses births beside the exhaust.

ring per generation, twice the speed of the published glider, verified flat to radius 384; its seed emits two gliders separated by $142.9° \approx 4 \times 36°$. Its automaton is Table 2, printed verbatim from the evolved genome in the convention of Section 6. The remaining finds are *wanderers*: cohesive, ash-free patterns of 17 to 32 cells whose displacement grows as t^α with $\alpha \approx 0.6$–0.85, roughly thirty times farther than diffusion over the measured span but short of ballistic, realized as straight runs along pentagrid directions punctuated by stochastic reorientation. Two further full-fitness champions were correctly rejected by verification, one locking into an exact period-145 orbit after 128 rings, one dying at 48. The rediscovery also calibrates search cost: the searches behind the negative result (Section 5.5) ran nearly an order of magnitude below the threshold at which gliders become findable on a substrate known to contain them.

5. Gliders on the Monotilings

5.1 Discovery

The pipeline of Section 4 was pointed at the monotilings unchanged: vertex neighborhood (measured fan margin two), four-state priority-table rules, random initialization, the same neutral seed bank, the same fitness (equation (1)) with population cap 64, searched at radius 48 with population 256 for 800 generations — the budget at which gliders are routinely findable on the Penrose rhomb tiling. Three independent runs were made on each family.

Four of the six runs produced cross-radius-verified gliders: three on

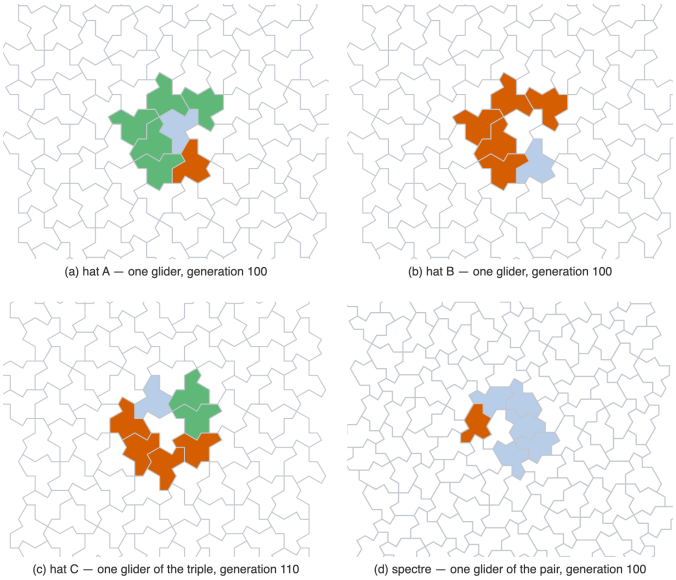

Figure 2. The four monotile gliders, one object each at a common scale — the glider body is the rule's invariant, shared by every seeding, while launch multiplicities and spread patterns are seed artifacts. (a) Hat glider A, a compact object of five to seven cells, at generation 100; (b) hat glider B at the same generation — visibly a different anatomy (its active cells alternate sides across the movement axis), yet it travels with the identical clock and heading as A; (c) one glider of hat C's triple at generation 110, shortly after the wandering intermediate decayed; (d) one glider of the spectre pair at generation 100 — the most minimal anatomy found, a single bright head and its wing wake. Colors as in Figure 1.

the hat and one on the spectre. Where the Penrose rediscovery had required about 1.15×10^5 genome evaluations to cross its needle, the first hat run reached full fitness at genetic generation five — roughly 1,300 evaluations. The two remaining runs were rejected by verification, and both rejections are instructive; they are discussed below. Figure 2 shows the four objects. Their complete automata and seeds, each with a space-time rendering and a full-lifetime trail, are collected in the atlas of Section 6; the rule behind Figure 1 appears there as Table 7.

5.2 Verification and the shared clock

Figure 3 shows the verification data. Each glider was replayed on monolithic patches of radius 48, 96, 192, 384, and 768 — a sixteenfold span, the largest a patch of about two million tiles — and reached

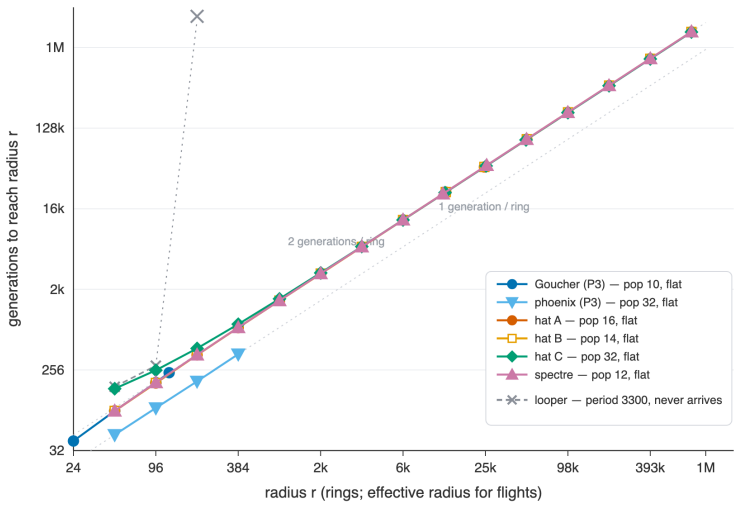

Figure 3. Generations to reach graph distance r from the seed, versus r, log–log. Points up to radius 768 are monolithic boundary arrivals; beyond, each line continues as a sliding-window flight plotted against effective radius, to one million rings. A glider is ballistic: slope one. All four monotile gliders share the clock of two generations per ring and fuse into a single bundle across more than three decades; the phoenix runs at one generation per ring. Arrivals are noisy at launch and converge onto the clock within a few hundred generations. The gray dashed curve is the rejected looper: at radius 192 both its wanderers are captured by closed loops (periods 60 and 550; full-state recurrence 3,300) and it never arrives (Section 6).

the boundary at every radius with its peak population exactly flat: 16, 14, 32, and 12 cells respectively, at every scale. Each was then flown by sliding window (Section 2.4) to one million rings — roughly 1,300 times the monolithic ceiling — with the same flat population and the same clock throughout, every hop an independently replayable record. The terrain crossed is never revisited, and the sequence of local environments along the lane, though its members recur, never becomes periodic.

The slopes carry a regularity that nothing selected for: the fitness functions reward directed travel with flat population and say nothing about speed. Yet five unrelated rules — Goucher's, designed by hand fourteen years earlier, and hat A, hat B, hat C (after its transient), and the spectre pair, evolved here — share a single clock of two generations per ring across three substrates, with the phoenix at exactly one. We

read the common value as the natural pace of relay transport: these objects do not translate but are re-formed ahead of themselves, and one ring of progress appears to cost one excitation–promotion cycle of the relay. The clock is predictive out of sample: fitted at radii up to 384, it puts the radius-768 arrivals near generation 1,536, and the measured values are 1,533–1,534.

What these verifications do and do not establish must be stated plainly. On a periodic lattice, gliderhood has a finite certificate: a pattern that recurs translated is immortal by symmetry. Goucher's glider has a geometric substitute (monotone progress along a ribbon). Neither is available here, and no finite replay can prove immortality on an aperiodic substrate; *glider* in this paper is the operational term defined by the verification standard, not a proven property. The in-family cautionary case is the spectre looper of Figure 3: its pair of wanderers traveled with near-flat population (29 rising to 31), one reaching ring 189 before being captured by a closed loop at generation 992 — so late transitions are real, and the million-ring flights stand more than three decades beyond the deepest capture observed. Two measured properties argue specifically against a hidden loop or late trap: loopers turn, while these gliders hold their settled headings to within hundredths of a degree over the entire flight (Section 5.4); and their arrival laws are predictive out-of-sample, where an approach to a loop would bend them. A path toward genuine proof is discussed in Section 7.

5.3 Launch, interactions, and ignition

Launch multiplicity is a property of the seed, not the rule: the heading sweep of Section 5.4 later found clean single-glider two-cell seeds on every hat spoke, and on most spectre lanes. The champion seeds, as it happens, all launch more than one object. Hat A's emits two gliders that travel together, braided a few tiles apart, until one strikes the other's wake at generation 42 and dies, leaving the survivor to run indefinitely. Hat B launches the same way. Hat C ignites through a bound intermediate: a wanderer that meanders near the origin before decaying into two, then three gliders; its 62-generation arrival offset is the cost of this phase. The spectre seed emits a clean pair separating onto lanes 120° apart. Figure 4 renders hat A's launch as space-time geometry.

Ignition does not depend on the discovery site. Seeding each rule's state pair across every shared edge of one interior anchor per tile class, in both orders, launches a verified-signature traveler from 71–89% of seedings (hat A 167 of 188; hat B 165 of 188; spectre 81 of 114). Goucher's rule scores 100% on this test, but unsurprisingly so: a head-and-tail pair is that glider's own small phase, so the seed is already a glider mid-cycle, and every P3 edge lies on a ribbon that supports

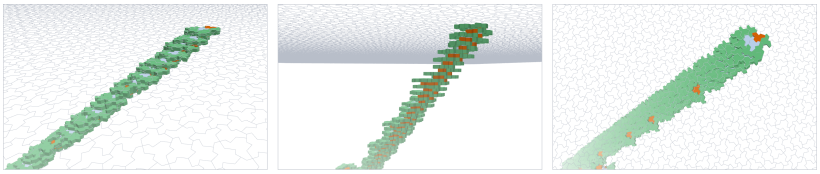

(a) oblique, above the present plane (b) from below the plane (c) overhead

Figure 4. Hat glider A's history as space-time geometry: each generation extrudes the non-quiescent tiles as prisms, time upward, older layers fading over 120 generations; the wireframe is the tiling at the current slice. (a) Oblique view from above the present plane; (b) from below — the state-1 footprints tick at exactly two generations per ring, the relay clock as visible rungs, with the launch transient the kink at the tube's foot; (c) overhead. Speed is slope, the generation-42 collision is a vertex where one tube ends on the other, and the tube's lean never leaves its compass direction. Rendered by the same engine that runs every figure live in the companion essay.

the next step. The monotile seeds match no settled configuration — the gliders fly at populations of six and above — so their percentages measure something stronger: the reach of the gliding attractor from arbitrary two-cell states. Strikingly, not one of roughly 490 seedings of those three rules died or froze — everything travels. Hat C ignites less often (45 of 188), consistent with its wanderer-mediated launch; visual review resolved most of its remaining seedings as multi-glider showers rather than growth, so the percentages are lower bounds. Beyond the launch annihilation, pairs at other sites interact *nondestructively*: course changes for one or both gliders, always settling at mutual separations of 60°, 120°, or 180°. The interaction repertoire — synthesis by pair launch, annihilation by wake contact, deflection onto compass-commensurate headings — is raw material for any future collision engineering.

5.4 The compass law

Every mobile object in this paper travels along directions quantized to its substrate's orientational order. On Penrose P3, measured by windowed segment fits at patch scale, Goucher's glider locks to the tenfold pentagrid fan to 0.08° mean windowed residual and the phoenix pair to 0.45°, separated by $142.9° \approx 4 \cdot 36°$; the coarser residuals reflect the short baseline, not a weaker lock — the Penrose objects were not reflown at flight scale. On the monotilings the flights measure the law at three more decades of baseline (Figure 5): settled headings on all six spokes of each substrate's sixfold fan — twelve lanes, found by binning generic-seed launches by heading — every one agreeing with a single per-substrate offset, hat 45.523° and spectre 48.014° in

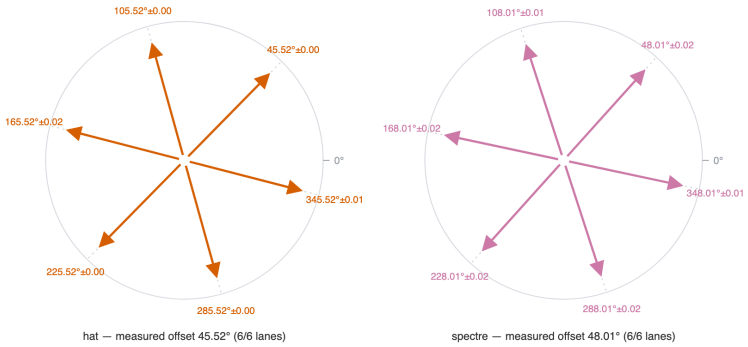

Figure 5. Flight-measured lane headings on the hat and spectre (arrows; settled heading with standard error, from the sliding-window flights). Every one of each substrate's six fan spokes carries a measured glider lane, and all twelve headings agree with a single per-substrate fan offset — hat 45.523°, spectre 48.014° — within standard errors of 0.001°–0.024°; lane separations are parameter-free multiples of 60°. Wanderers are omitted: their run segments lock to the fan, their net drift — a sum over reorientations — does not.

the canonical frame of the root tile, within standard errors of 0.001°–0.024°. Separations between lanes are parameter-free: the hat triple's $120.001° \pm 0.011°$, the spectre pair's $240.000° \pm 0.009°$ — multiples of 60° to within a hundredth of a degree. Even the Penrose *wanderers* — cohesive, ash-free movers whose displacement grows as t^α with $\alpha \approx 0.6$–0.85 — obey the law in segments: their straight runs lock to the pentagrid fan at short windows, with stochastic reorientation between runs, so the substrate sets the transport law while the rule sets the reorientation rate.

Launch transients — start-point offsets and early reorientations — decay as $1/r$, and the heading sweep caught one launch mid-capture: it ran four window-hops near one spoke, reoriented by exactly 60° in a single hop, and held the adjacent lane for the remaining hundred thousand rings (the record replays in the interactive essay). Lane-locking, on this evidence, is an attractor process: the six spokes are attracting states of the relay, a transient can include a whole lane switch, and no settled glider has ever been observed to leave its lane.

Figure 6 shows the approach to the fan. Running headings converge as $1/r$ — the launch transient's start-point offset averaging out — and there is no residual floor: beyond roughly thirty thousand rings every lane's residual is statistically zero, with standard errors

	Edge adjacency	Vertex adjacency
Generations ($k = 4$)	mortal travelers, 43–58 rings	mortal travelers, 45–58 rings
Priority tables	mortal travelers and oscillators, 31–47 rings	**gliders (four of six runs)**

Table 3. The ablation grid at the calibrated search budget. The edge-adjacency Generations cell reproduces the negative result at thirteen times the budget of the searches that established it, so that null was not underpowered. All three null cells share the same ceiling — mortal travelers of roughly 30–60 rings — and only the combination of vertex neighborhood and neighbor-visible rule states crosses from mortal to verified gliding.

of 0.003°–0.011° at one million rings, corresponding to about fifty tiles of transverse drift over the entire flight. The lanes are real objects with measurable widths: Goucher's ribbon-guided glider deviates less than one tile from a straight line over a hundred tiles, while the monotile gliders, with no rail beneath them, hold lanes two to four tiles wide. Rails, on this evidence, were never the requirement for directed transport — the orientational order that every substitution tiling carries suffices to steer, and the Penrose ribbons are simply the case in which the lane is rigid.

The fan's phase — why 45.523° — is itself substrate geometry. The graph-metric ball of each tiling is a rounded hexagon, far from circular: Euclidean reach per ring varies with direction by 15% on the hat and 12% on the spectre, peaking in six sharp cusps. Locating the cusps by flank intersection on a radius-384 patch places all twelve, six per substrate, at the measured lane directions to within 0.15°, with the reach at each cusp matching the flights' rings-per-length constant to a few parts per thousand. The gliders travel the fast axes of their substrate's metric, at the metric rate: the compass phase is a constant of the tiling, not of the rule. (Chaotic growth fronts, by contrast, are circular to about 1% on these same tilings — growth is dynamically smoothed and does not probe the cusps.)

5.5 The ablation

Section 4 identified two extensions to the originally searched space: the vertex neighborhood, and rules whose non-quiescent states are visible to neighbors under conjunctive conditions. To attribute the gliders, the full two-by-two grid was searched at the calibrated budget — two independent runs on each family per cell, each cell searched by its established machinery. Table 3 gives the outcome: both extensions are individually necessary, and only their combination suffices.

The null cells are informative beyond attribution. Generations rules fail on both neighborhoods, even searched with per-class stratified tables: their dying states are invisible to neighbors, so the extra adjacency of the vertex neighborhood adds nothing such a rule can read.

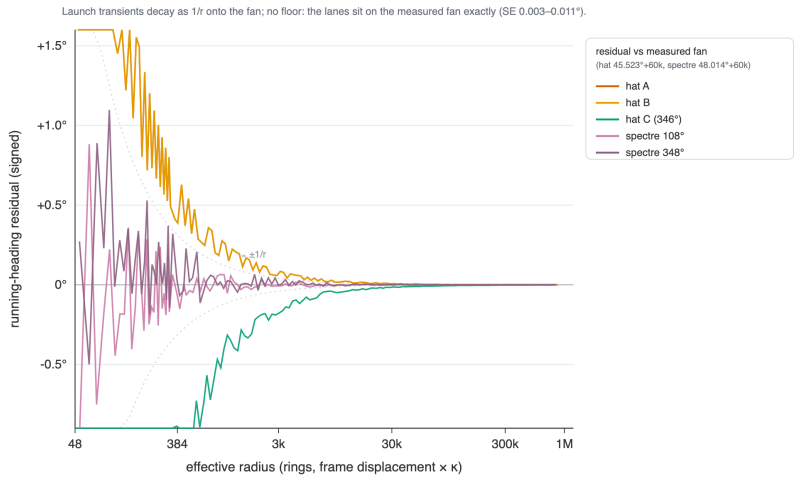

Figure 6. Signed residual of the running heading from the nearest spoke of the measured fan, versus effective radius. Launch transients decay as $1/r$ (dotted envelopes) onto the fan; beyond about thirty thousand rings every lane's residual is statistically zero. Three hat gliders from independent genomes — two sharing a lane, the third 120° away — and both members of the spectre pair (240° apart) land on the same per-substrate fan. Hat A lies exactly beneath hat B; hat C's larger transient is its wanderer-mediated launch.

On the square lattice the same semantics are glider-prolific — Brian's Brain is the $k = 3$ Generations rule $B = \{2\}$ with empty survival [17] — so the failure is a property of the pairing with aperiodic ground, not of the family. Priority tables fail on edge adjacency even though the rule family provably contains relay mechanisms. And all three null cells plateau at the same 30–60-ring mortal ceiling that every search in the deficient spaces runs into, exhaustive or evolutionary, on either family — suggesting that the ceiling is a property of the rule spaces, not of the tilings, which the fourth cell confirms. The search in that cell also produced a fourth fitness parasite, *boundary sniffing* (Section 3), whose structural fix, the causality filter, is inherited by every search reported here.

6. An Atlas of the Monotile Gliders

This section gives, for each of the four gliders and then for the looper that the verification standard rejected, everything needed to recreate and recognize it: the complete automaton, verbatim from the evolved genome, with inert rows grayed out — a row is grayed when deleting it leaves every configuration of the verified replay unchanged, so the black

Current state	Neighbor condition	Next state
0	$n_2 \geq 2$	0
any	$n_1 \geq 3$ and $n_1 \geq 1$	3
2	$n_1 \geq 1$ and $n_0 \geq 1$	1
1	$n_2 \geq 1$ and $n_2 \geq 1$	3
2	always	0
0	$n_1 \geq 1$	2
2	$n_3 \geq 2$	0
2	always	0
any	otherwise	0

Table 4. Hat glider A's automaton (first matching row fires). The grayed rows are inert: all three send state 2 to quiescent, which is the default fall-through.

rows are the working rule and the gray are genetic cruft (duplicated conjuncts, shadowed rows), reproduced because the record is the rule; the final row of each table is the default — a close-up of the object in flight, an oblique space-time rendering (conventions of Figure 4: tiles extrude upward in time, 120- generation fade, wireframe at the present), and the full lifetime of the discovery run replayed at radius 384 — an overhead map in which every tile that was ever non-quiescent is tinted by the time of its first activation, from pale sand at launch to vermilion at the boundary, with the final generation in the state palette and the patch edge drawn as the surrounding ring. Colors follow Figure 1 throughout. Every panel regenerates from the committed records.

A *situation* is a snapshot of the glider as the rule sees it: the non-quiescent cells together with the substrate *collar* within a fixed graph radius of them — tile classes, adjacencies, and vertex degrees — canonically encoded, so that two snapshots are equal exactly when their collared neighborhoods are isomorphic, wherever on the tiling they occur. The *flying vocabulary* is the number of distinct situations an object occupies over its verified flight; Section 7 builds on the finiteness of this set.

6.1 Hat glider A

Record `hat-tableevolve-r48-s21`: peak population 16, two generations per ring, settled heading 225.523° (a spoke of the sixfold fan), launched by seeding states (1, 2) across one shared edge at the patch root; 89% of arbitrary two-tile seedings of this rule launch travelers, and none die. Its flying vocabulary is 167 situations. The trail (Figure 7c) records the launch: two gliders braid from the seed until one dies on the other's wake at generation 42 — the short stub at the pale end of the ribbon — and the survivor flies straight, meeting the boundary exactly at the southwest corner of the patch.

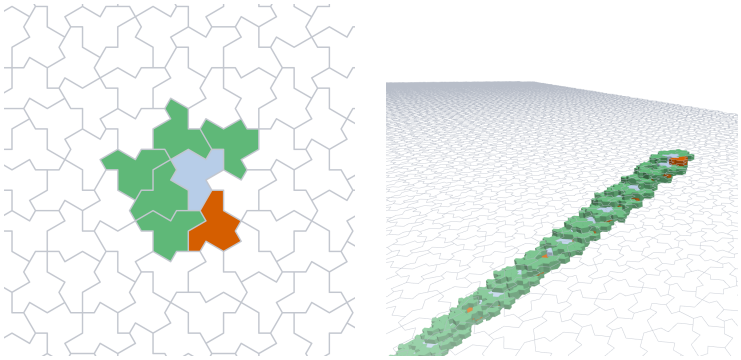

(a) (b)

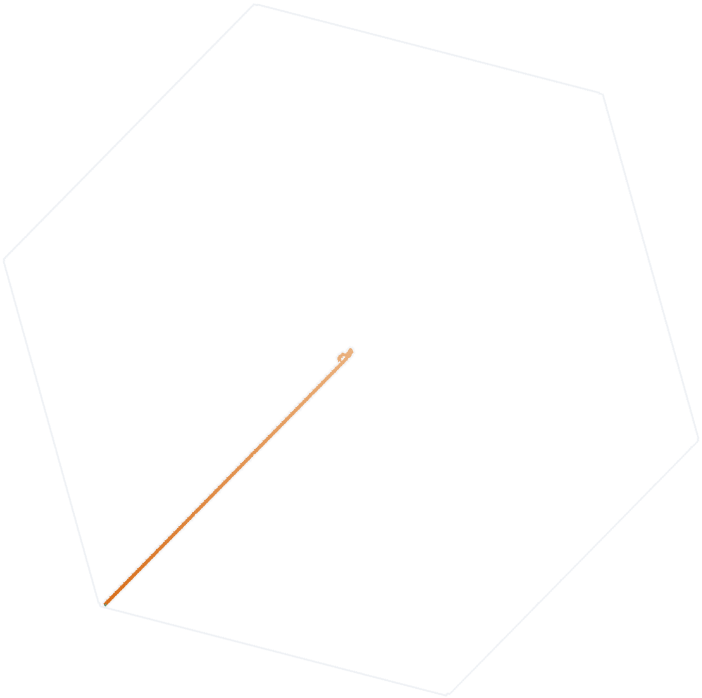

(c)

Figure 7. Hat glider A. (a) In flight at generation 100. (b) Space-time world-tube, frozen at generation 150 mid-cruise. (c) Full lifetime at radius 384: 759 generations, 1,942 tiles visited; the pale curl at the ribbon's start is the two-glider launch and generation-42 collision, and the ribbon meets the boundary at a corner of the patch — the compass law drawn by the object itself.

Current state	Neighbor condition	Next state
0	$n_1 \geq 2$ and $n_0 \geq 1$	0
0	$n_0 \geq 2$ and $n_2 \geq 2$	1
0	$n_0 \geq 2$ and $n_3 \geq 1$	1
1	$n_3 \geq 1$	3
any	otherwise	0

Table 5. Hat glider B's automaton — the tersest glider rule found. State 1 has no survival row: a bright cell lasts one generation, becoming a wing if a wing stands beside it and dying otherwise, so the anatomy is reborn ahead at every step. The grayed row waits for state 2, which neither the seed nor any row produces: it can never fire.

Current state	Neighbor condition	Next state
any	$n_2 \geq 1$ and $n_1 \geq 3$	3
1	$n_2 \geq 1$	2
3	$n_3 \geq 3$	3
0	$n_3 \geq 2$	1
any	$n_2 \geq 1$	1
1	$n_0 \geq 3$ and $n_2 \geq 2$	2
0	$n_3 \geq 3$	3
any	otherwise	0

Table 6. Hat glider C's automaton. The grayed rows are inert, each shadowed by an earlier row: six by two (same outcome), seven by four, which fires first on every cell seven matches.

6.2 Hat glider B

Record `hat-tableevolve-r48-s22`: peak population 14, and the same clock, heading, and windowed-heading sequence as hat A — one phenotype in two genomes — but a different anatomy (four to five state-1 cells alternating sides across the movement axis, where A carries a state-2 body) and the tersest rule found: three working rows. Seed (3, 1); ignition 88%, none die. Its launch also emits a braided pair with one survivor, visible as the stub in Figure 8c.

6.3 Hat glider C

Record `hat-tableevolve-r48-s23`: the wanderer-mediated triple. The seed (2, 1) ignites a bound intermediate that meanders near the origin before decaying into three gliders — a parallel pair on the 105° lane and a third on 345°, a separation of $2 \cdot 60°$. Peak population 32 across all three; arrival law $\mathrm{gen}(r) = 62 + 2r$; ignition 24% (most other seedings launch multi-glider showers through the same intermediate). The trail (Figure 9c) shows the central knot of the wandering phase and the two ribbons leaving it.

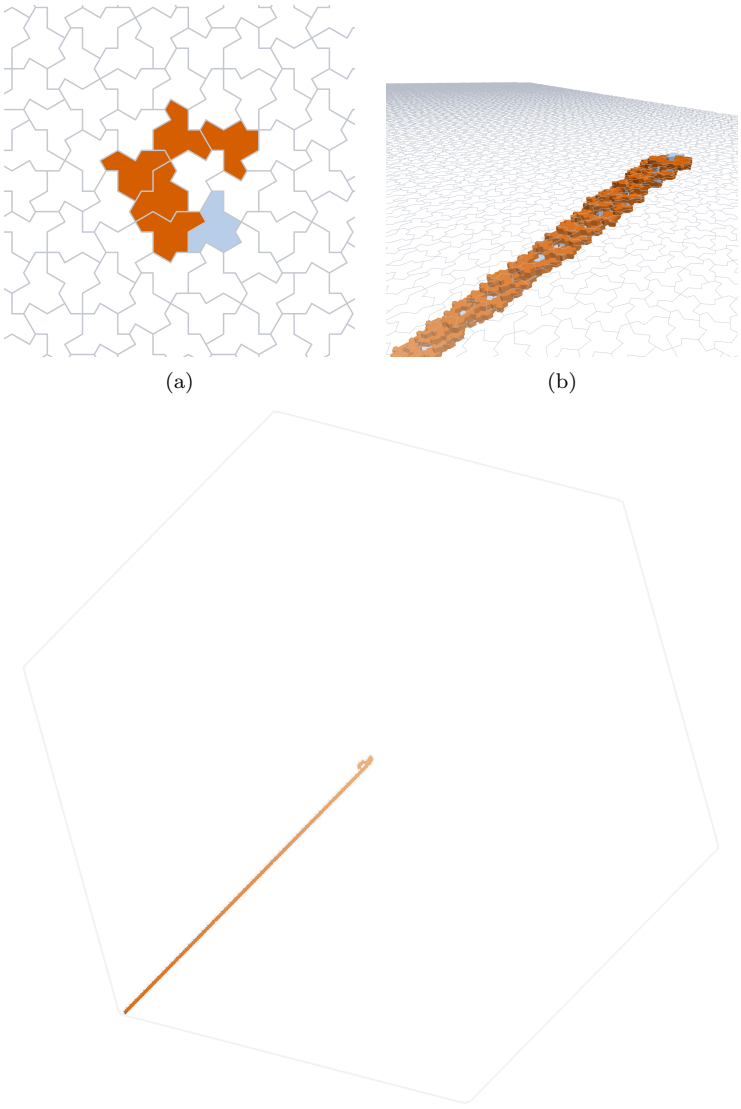

Figure 8. Hat glider B. (a) In flight at generation 100 — the state-1-heavy anatomy, visibly unlike A's. (b) Worldtube at generation 150. (c) Full lifetime at radius 384: same launch stub, same corner, same clock as A, from an unrelated genome.

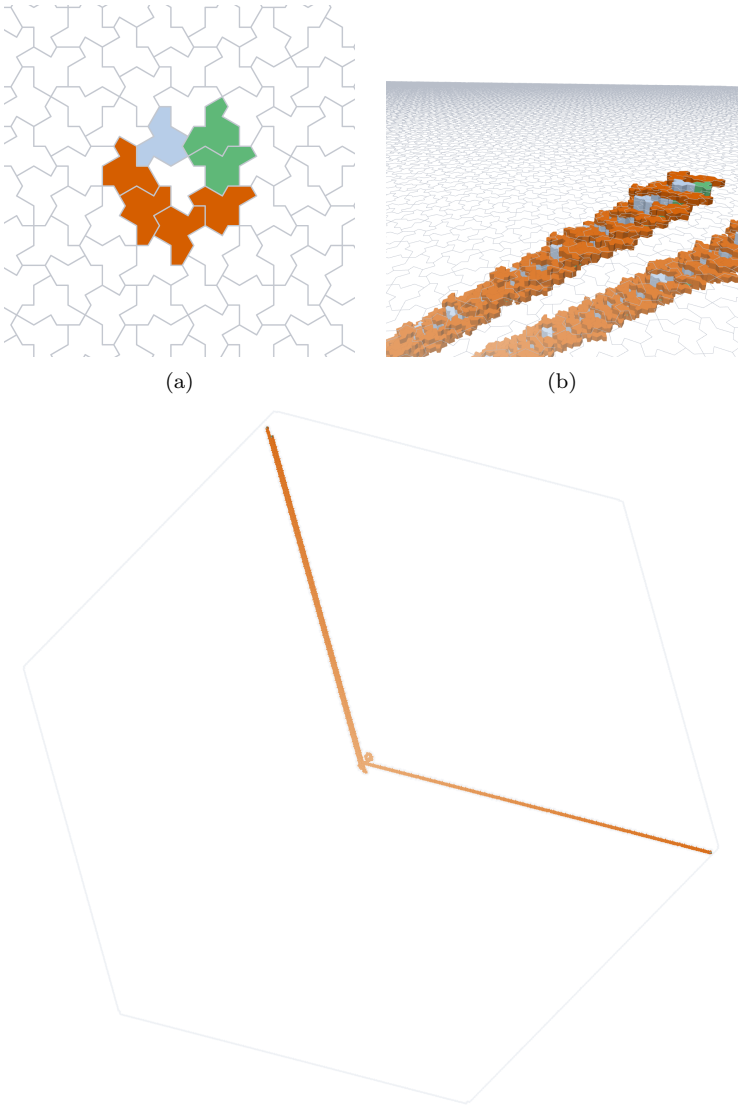

(a) (b)

(c)

Figure 9. Hat glider C. (a) One glider of the 105° pair at generation 110. (b) Worldtube of the parallel pair at generation 175 — two tubes climbing side by side. (c) Full lifetime at radius 384: 830 generations, 5,167 tiles visited; the central knot is the wandering intermediate, and the two ribbons — the merged parallel pair east-southeast and the lone glider north-northwest — open onto lanes 120° apart.

Current state	Neighbor condition	Next state
0	$n_0 \geq 3$ and $n_1 \geq 1$	3
0	always	0
3	$n_3 \geq 3$	0
0	$n_0 \geq 3$ and $n_1 \geq 1$	0
3	$n_1 \geq 1$	1
0	always	0
any	otherwise	0

Table 7. The spectre glider's automaton, the rule behind Figure 1 (first matching row fires). The grayed rows are inert: row two restates the quiescent default and rows four and six sit in its shadow; the only live ground transition is row one.

6.4 The spectre glider

Record `spectre-tableevolve-r48-s33`: mechanically the most minimal of the four — a pure three-state relay that never enters state 2 (Table 7: a head excites wings; a wing beside a head is promoted to the next head; crowded wings die). Seed (1, 3); the pair separates onto lanes 120° apart; peak population 12 for both gliders; the tightest compass lock measured (settled heading within 0.006° of the fan over a million-ring flight); ignition 71%, none die. Its flying vocabulary is 306 situations.

6.5 The spectre looper

Record `spectre-tableevolve-r48-s32` is the atlas's counterexample — the object the cross-radius standard rejected, and the reason the standard matters. Its seed (3, 1) launches a pair of oscillating wanderers with peak population 29–31; it reached full fitness in its search and passed the radius-48 and radius-96 replays. At radius 192 the classifier reports an exact recurrence of the full patch state with period 3,300 — the longest observed in this project — but that number is the beat of two independent captures, not any single orbit. One wanderer is trapped almost at once: at generation 92 it locks into a period-60 loop, a 207-tile track on rings 17–40. Its twin wanders for a thousand generations, reaching ring 189, before locking at generation 992 into a period-550 circuit — a closed track of 1,509 tiles spanning rings 107–189 — and from that moment the full state is periodic with period $\mathrm{lcm}(60, 550) = 3300$. At the anatomy scale (Figure 11a) it is indistinguishable from a glider. The lifetime views are what separate it: where every glider in this atlas draws a straight ribbon into a corner of the patch, the looper's trail (Figure 11c) wanders from its first generation — it never had the straight-lane signature — and ends in two closed orbits, the patch boundary far beyond the frame. Its worldtube snakes where the gliders' tubes climb straight.

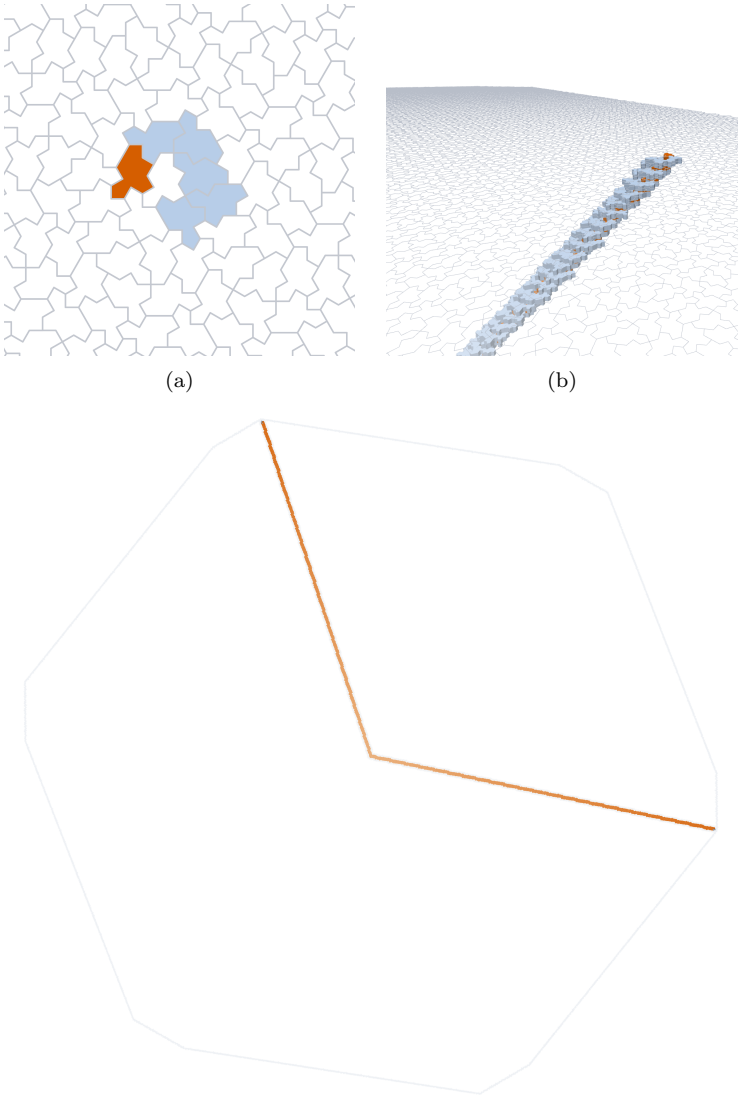

Figure 10. The spectre glider. (a) One glider of the pair at generation 100 — a single head cell and its wing wake. (b) Worldtube at generation 150, following one glider. (c) Full lifetime at radius 384: 761 generations, 3,435 tiles visited; the two ribbons leave the seed on lanes 120° apart and both reach the boundary.

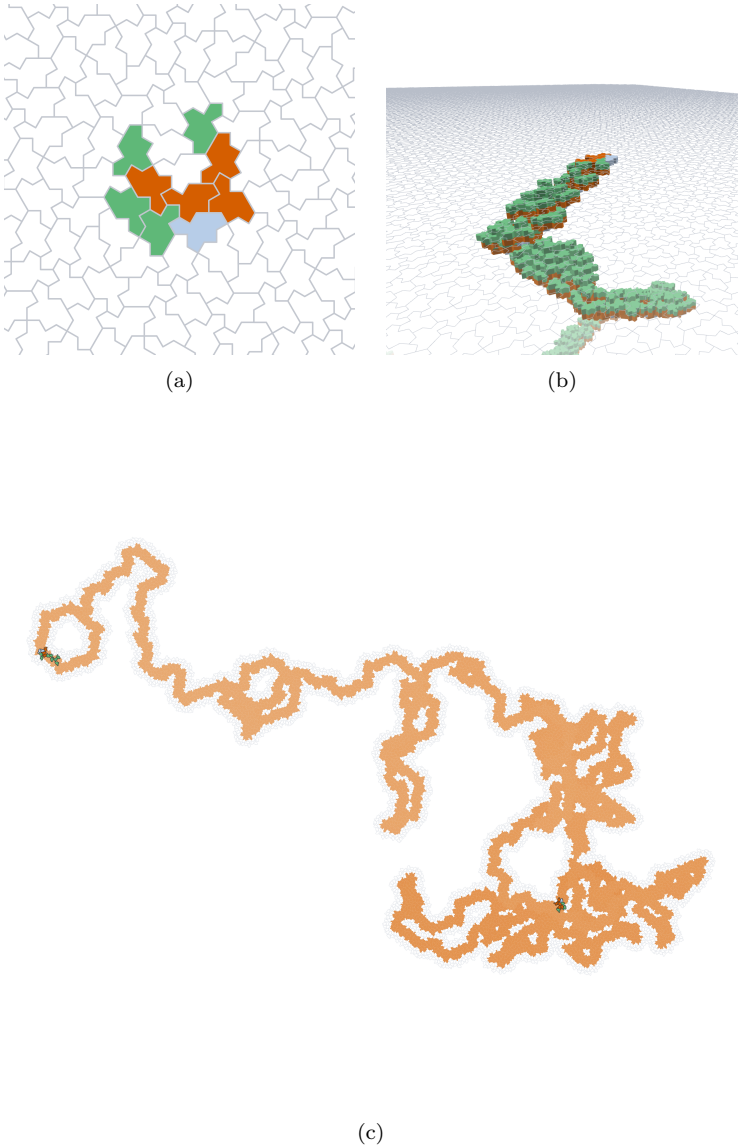

(a) (b)

(c)

Figure 11. The spectre looper. (a) At generation 100 — indistinguishable from a glider at this scale. (b) Its worldtube snakes and doubles back where a glider's climbs straight. (c) Full lifetime over 4,800 generations at radius 384 (4,534 tiles visited), zoomed to the trail: the pair separates at once; one wanderer is trapped by generation 92 in the period-60 loop visible in the state palette near the pale launch end, while its twin meanders for a thousand generations before settling onto the period-550 circuit threading the dense tangle at lower right. The patch boundary the gliders reach lies far outside this frame.

Current state	Neighbor condition	Next state
0	$n_1 \geq 1$ and $n_3 \geq 1$	3
0	$n_1 \geq 1$ and $n_3 \geq 1$	3
0	$n_0 \geq 2$ and $n_3 \geq 1$	1
1	$n_0 \geq 2$	2
0	$n_2 \geq 3$	2
1	always	1
3	$n_3 \geq 1$	1
3	$n_0 \geq 1$	1
any	otherwise	0

Table 8. The spectre looper's automaton. The grayed rows are inert: row two duplicates row one, and every conversion row seven would make, row eight makes identically.

7. Discussion

The contrast between the Penrose gliders and the monotile gliders localizes what directed transport actually requires. Goucher's glider is guided by a geometric rail whose parallelogram monotonicity also supplies its immortality proof, and it holds its lane to within a tile; the monotilings offer no rails, and their gliders wander in corridors two to four tiles wide on the radius-384 trails while holding heading to thousandths of a degree over a million rings — quantization equally sharp on both substrates. What the substrates share is not rails but orientational order: a substitution tiling carries a globally coherent orientation field, hierarchically propagated, with finitely many tile orientations, and this compass evidently suffices to steer a relay. On this reading the de Bruijn ribbons are the special case in which the compass comes with a rigid lane, and the natural conjecture is that any substitution tiling supports compass-locked gliders once its rule space is expressive enough in the sense of the ablation. The lanes lie on the measured fan exactly, and the fan is the cusp structure of the graph metric — the compass phase is substrate geometry. Deriving that phase is now the open problem: the cusps sit 15.5° (hat) and 18.0° (spectre) from the tile-edge direction classes, on no crystallographic grid, and their closed form plausibly lives in the tilings' cut-and-project descriptions: each tiling has a model-set representative in its conjugacy class, with pure-point diffraction computed explicitly [18, 19, 20]. One suggestive agreement deserves recording. The hat offset matches $180° - 2\theta^*$, where $\theta^* = \cos^{-1}\big(\sqrt{2}/(4\phi^2)\big)$, with ϕ the golden ratio, is the twist angle between the two hexagonal edge-direction families of the hat tiling's inflation-invariant limit geometry [18]: 45.5225° against the measured $45.523° \pm 0.003°$, with no adjustable parameter. A single-substrate match may yet be coincidence; the discriminating test is the spectre, whose analogue must emerge from the $4 + \sqrt{15}$ arithmetic of its model

set [20] with no further freedom. An exact computation of the inflation-limit edge directions, in the frames the flights were measured in, would decide it; we leave this to future work.

The taxonomy assembled across three substrates — gliders, wanderers, loopers — reads less like three kinds of object than one family in three regimes. Hat C's ignition shows a wanderer decaying into three gliders, direct evidence that wanderers are excited bound states of gliders; the Penrose wanderers travel in fan-locked ballistic segments between stochastic reorientations; and the loopers, from the kite-and-dart orbits to the spectre looper, are glider mechanisms whose paths close. The heading sweep even caught the intermediate live: one launch ran briefly on one spoke, reoriented once, and committed to the adjacent lane for a hundred thousand rings — a lane capture: a wanderer with exactly one segment boundary. The shared relay clock and the shared compass are the unifying measurements. In this picture the interesting variable is not whether a rule supports motion but which regime the motion lands in — open lane, reorienting walk, or closed orbit — a classification reminiscent of the search-discovered mobile objects of continuous cellular automata [21], here with the substrate's geometry supplying the classifying structure.

Prospects for engineering must respect what aperiodicity removes. It does not remove computation: a six-state semi-totalistic automaton on the kite-and-dart tiling already simulates any boolean circuit and any Turing machine [22]. What it removes is the economics of construction. Constructive universality in the Game of Life rests on components that, verified once, work everywhere, translation symmetry making every site equivalent; the same guarantee underlies glider-based universality in cellular automata generally [23]. Here no symmetry carries one site to another: a collision verified at one place holds only at the locally isomorphic recurrences of that exact configuration, scattered at substrate-chosen locations that must be found rather than reached by translation. Engineering would therefore need site search plus site-by-site verification, or components proven site-independent by a certificate argument of the kind sketched below.

The observed repertoire is nonetheless a real starting kit: reliable pair synthesis from two-cell seeds, annihilation by wake contact, nondestructive deflection, and settlement onto compass-commensurate mutual headings — the last suggesting that multi-glider configurations have a discrete, enumerable set of stable geometries, which is exactly what an engineer wants. The looper hints at the storage half of such a kit: it is the one object here whose immortality is proved rather than extrapolated (the exact cycle is a theorem about its patch), and its hexagonal period-60 loop alone is, in principle, five bits of phase. But the orbit is committed to the specific environment its wanderer happened to find — local isomorphism guarantees such sites recur with

bounded density, though not where — and it inhabits a different rule from the spectre glider, so the prerequisite for any signal-plus-storage program is an object census within a single rule. An alternative road avoids free flight altogether: signals confined to constructed channels, in the manner of von Neumann's original automaton [13], would trade the compass problem for a plumbing problem and deserve their own search.

The limitations are those already stated, plus scope. Immortality is empirical, with the certificate problem open. The ablation's null cells are bounded by budget — two runs per family per cell — and assert difficulty, not emptiness. The rule space searched is four-state semi-totalistic priority tables, a thin slice of local rules. Discovery ran from a single root per family (ignition genericity covers launch sites, not root choices). And every object here was found by one fitness function; the searches were stopped by success, not exhaustion, so the taxonomy is surely incomplete.

Future work is led by the certificate problem: can *verified to a million rings* be upgraded to *immortal on every legal tiling*? Substitution tilings have finite local complexity, and one step of a cellular automaton is strictly local, so a proof reduces to closure: enumerate the situations a flying glider occupies — its states together with the canonical collar graph, degrees included — and show the set closes under the step map, with positive displacement, for every collar extension. Two structural gifts make this tractable. Over-approximating the legal extensions is safe (survival on a superset proves survival on the tiling), so the substitution hierarchy is needed only where a lazy enumeration fails; and the compass lane reduces the terrain ahead to a corridor whose collar sequence is itself substitutive, making the certificate a product of the glider's phase machine with a finite corridor automaton — the ribbon proof reappearing as the one-letter special case.

We have run the decisive first experiment: the count of distinct situations versus generation, with a cross-radius determinism control validating the encoding (the same-collar successor map is not forced even by a perfect encoding, so soundness is checked on the forced maps from larger collars to smaller successors, all of which are deterministic). The hat A glider occupies exactly 167 distinct situations at the step-sufficient collar radius. The last new situation appears at generation 434; on the doubled patch, 1,074 consecutive further generations of entirely fresh terrain produce nothing new. Branching — situations with more than one observed continuation — is confined to four situations with two continuations each, and their recurrence gaps carry the additive structure of a substitutive sequence. The spectre glider gives the same picture with a vocabulary of 306. Vocabularies are per-lane: the lane-capture trajectory shares not one situation with the canonical glider's atlas, even while visually indistinguishable from it, so a cer-

tificate covers one rule–lane pair and six certificates cover a substrate. And because semi-totalistic dynamics are blind to the tile classes the keys record, the designated first step is a class-blind encoding: if the six lanes' machines coincide there, as their identical clocks and speeds suggest, each certificate factors into a small phase machine crossed with a per-lane corridor automaton. The certificate is therefore no longer a conjecture about whether a finite description exists — it measurably does — but a bounded enumeration task: generate the legal collar continuations of these situations from the substitution hierarchy and verify closure of the graph. Beyond the certificate: five and more states and per-class stratified tables (is there a faster monotile glider?); a deliberate collision study built on the interaction repertoire; run-length statistics of wanderer segments, to locate what sets the reorientation rate; and the standing question of a Life-isomorphic automaton on the hat [10].

We close with a methodological remark. Nearly every substantive claim in this project was, at some stage, almost false: the searches invented four distinct ways to game their objectives, an early symmetry claim died under a planned control, and the published table we validated against contained a misprint. What made the surviving results stable was not caution but structure — pre-stated kill-conditions, controls run before claims were recorded, and every parasite promoted into a permanent filter. We offer the workflow, in the tradition of open systematic exploration of simple programs [24], as a result alongside the results.

Note added. After the first version of this paper was posted, Andrew Trevorrow pointed out his *HatLife* [11]: an interactive environment, announced in May 2023, that runs Generations-style and hand-designed rules on a fixed patch of 21,781 hats, with a spectre companion since. That version claimed that no cellular automaton on either tiling had previously been reported. The claim was wrong and is withdrawn. HatLife's exploration found oscillators, a WireWorld implementation, and a four-state rule designed so that chains called *worms* travel the corridors between rows of reflected hats, which the rule holds permanently empty; its body, head, and tail states are all visible to neighbors, so it is a priority-table rule in the sense of Section 3 on the vertex neighborhood, the one cell of the ablation of Section 5.5 in which gliders were found. Those worms are gliders in the sense of this paper. Transcribed into the present machinery (vertex neighborhood; a two-stratum table rule, the reflected hats given a table with no rows), worms arise from random soups as Trevorrow reported, and two of them, of population eight and seven, kept population and extent unchanged on patches of radius 48, 96, 192, and 384 while traveling, at two generations per ring, to the boundary of each: the cross-radius criterion of Section 3. Their corridors are not the rails of Section 1: the reflected hats mark

a direction, but nothing confines a worm to it, and the worms wander within their corridors as the gliders of this paper do. Their headings, measured at patch scale as for the Penrose objects of Section 5.4, are 225.524° and 45.519°, on the hat compass of that section to a few thousandths of a degree, the fit's standard error: an out-of-sample test by a rule written by hand, for a different purpose, three years before the compass was measured. The transcription and its record are available from the author and will accompany a later release; they are not part of the archived release of Section 8. What this paper adds to that exploration is a searched rule space on either tiling, objects followed beyond any fixed patch, and the compass law.

8. Reproducibility

Everything reported here regenerates from a small artifact set. The source repository contains the engine, the search drivers, every committed result record, the object compendium, and the figure pipelines; each figure directory carries the script that regenerates it from the records; the repository is public at github.com/jamesedmond/monotile-ca and archived at Zenodo (doi:10.5281/zenodo.22836247). A run is a record of tiling family, root address, radius, neighborhood, rule, and seed, and every quantitative claim in this paper maps to a record file and a single command; for example, the radius-768 verification of hat glider A is one invocation of the verifier against its committed record. The million-ring flights regenerate the same way — one invocation of the sliding-window tracker against a committed seed record — and the repository carries each flight's decimated telemetry and its final checkpoint: the glider at its millionth ring, independently replayable.

The companion interactive essay presents the same records live at offlattice.org/monotile/essay/. The engine that ran every search is compiled unchanged to WebAssembly, so the browser replays are the evidence, not an illustration of it: each panel replays a committed record, offers the record itself for download, and displays the command that re-verifies it.

Three determinism properties underwrite the scheme. Patches regenerate exactly from their identifiers, with cell numbering stable under radius growth, so a seed recorded at radius 48 lands on the same tiles at radius 768. Searches are deterministic given their recorded parameters and seeds. And the search code and the browser run one code base, so verification and presentation cannot drift apart.

Acknowledgments

This work was carried out with substantial assistance from an AI coding agent (Claude, Anthropic), which implemented the toolchain and

searches and drafted analyses under the author's direction; all claims were verified by structural controls (pre-stated kill-conditions, cross-radius and causality checks) and by the author's independent review of the replayable records. Andrew Trevorrow pointed out his 2023 HatLife and corrected the priority claim of an earlier version of this paper.

References

[1] D. Smith, J. S. Myers, C. S. Kaplan, and C. Goodman-Strauss, "An Aperiodic Monotile," *Combinatorial Theory*, **4**(1), 2024. doi:10.5070/C64163843.

[2] D. Smith, J. S. Myers, C. S. Kaplan, and C. Goodman-Strauss, "A Chiral Aperiodic Monotile," *Combinatorial Theory*, **4**(2), 2024. doi:10.5070/C64264241.

[3] M. Gardner, "Mathematical Games: The Fantastic Combinations of John Conway's New Solitaire Game 'Life'," *Scientific American*, **223**(4), 1970 pp. 120–123.

[4] E. R. Berlekamp, J. H. Conway, and R. K. Guy, *Winning Ways for Your Mathematical Plays*, Vol. 2, London: Academic Press, 1982.

[5] R. Penrose, "Pentaplexity: A Class of Non-periodic Tilings of the Plane," *The Mathematical Intelligencer*, **2**(1), 1979 pp. 32–37. doi:10.1007/BF03024384.

[6] N. Owens and S. Stepney, "Investigations of Game of Life Cellular Automata Rules on Penrose Tilings: Lifetime, Ash, and Oscillator Statistics," *Journal of Cellular Automata*, **5**(3), 2010 pp. 207–225.

[7] A. P. Goucher, "Gliders in Cellular Automata on Penrose Tilings," *Journal of Cellular Automata*, **7**(5–6), 2012 pp. 385–392.

[8] A. Trevorrow. "Gliders Are Impossible in Penrose Tiling?" from the reaction-diffusion mailing list. (2012) groups.google.com/g/reaction-diffusion/c/XPPeD3zxsEY.

[9] N. G. de Bruijn, "Algebraic Theory of Penrose's Non-periodic Tilings of the Plane. I, II," *Indagationes Mathematicae (Proceedings)*, **84**(1), 1981 pp. 39–66.

[10] D. A. Bailey and K. A. Lindsey, *A Game of Life on Penrose Tilings*, 2017. arxiv.org/abs/1708.09301.

[11] A. Trevorrow. "HatLife," ConwayLife forum thread, May 2023, conwaylife.com/forums/viewtopic.php?t=6015; "SpectreLife," 2026, conwaylife.com/forums/viewtopic.php?t=7489. Scripts for the Glu environment, glu1.sourceforge.io.

[12] S. Tatham, *Finite-State Transducers for Substitution Tilings*, 2025. arxiv.org/abs/2512.16595. Software: crates.io/crates/substitution-tiling-transducers.

[13] J. von Neumann, *Theory of Self-Reproducing Automata* (A. W. Burks, ed.), Urbana: University of Illinois Press, 1966.

[14] E. F. Moore, "Machine Models of Self-Reproduction," in *Mathematical Problems in the Biological Sciences* (Proceedings of Symposia in Applied Mathematics, Vol. 14), Providence: American Mathematical Society, 1962 pp. 17–33.

[15] R. P. Brent, "An Improved Monte Carlo Factorization Algorithm," *BIT Numerical Mathematics*, **20**(2), 1980 pp. 176–184. doi:10.1007/BF01933190.

[16] Ready, Release 0.x, GollyGang, github.com/GollyGang/ready.

[17] T. Toffoli and N. Margolus, *Cellular Automata Machines: A New Environment for Modeling*, Cambridge, MA: MIT Press, 1987.

[18] J. E. S. Socolar, "Quasicrystalline Structure of the Hat Monotile Tilings," *Physical Review B*, **108**, 2023 224109. doi:10.1103/PhysRevB.108.224109.

[19] M. Baake, F. Gähler, and L. Sadun, "Dynamics and Topology of the Hat Family of Tilings," *Israel Journal of Mathematics*, **270**(1), 2025 pp. 449–485. doi:10.1007/s11856-025-2780-8.

[20] M. Baake, F. Gähler, J. Mazáč, and A. Mitchell, "Diffraction of the Hat and Spectre Tilings and Some of Their Relatives," *Journal of Mathematical Physics*, **66**(9), 2025 092707. doi:10.1063/5.0264955.

[21] B. W.-C. Chan, "Lenia: Biology of Artificial Life," *Complex Systems*, **28**(3), 2019 pp. 251–286. doi:10.25088/ComplexSystems.28.3.251.

[22] K. Imai, T. Hatsuda, V. Poupet, and K. Sato, "A 6-State Universal Semi-totalistic Cellular Automaton on Kite and Dart Penrose Tilings," *Fundamenta Informaticae*, **126**(2–3), 2013 pp. 247–261.

[23] M. Cook, "Universality in Elementary Cellular Automata," *Complex Systems*, **15**(1), 2004 pp. 1–40.

[24] S. Wolfram, *A New Kind of Science*, Champaign, IL: Wolfram Media, 2002.